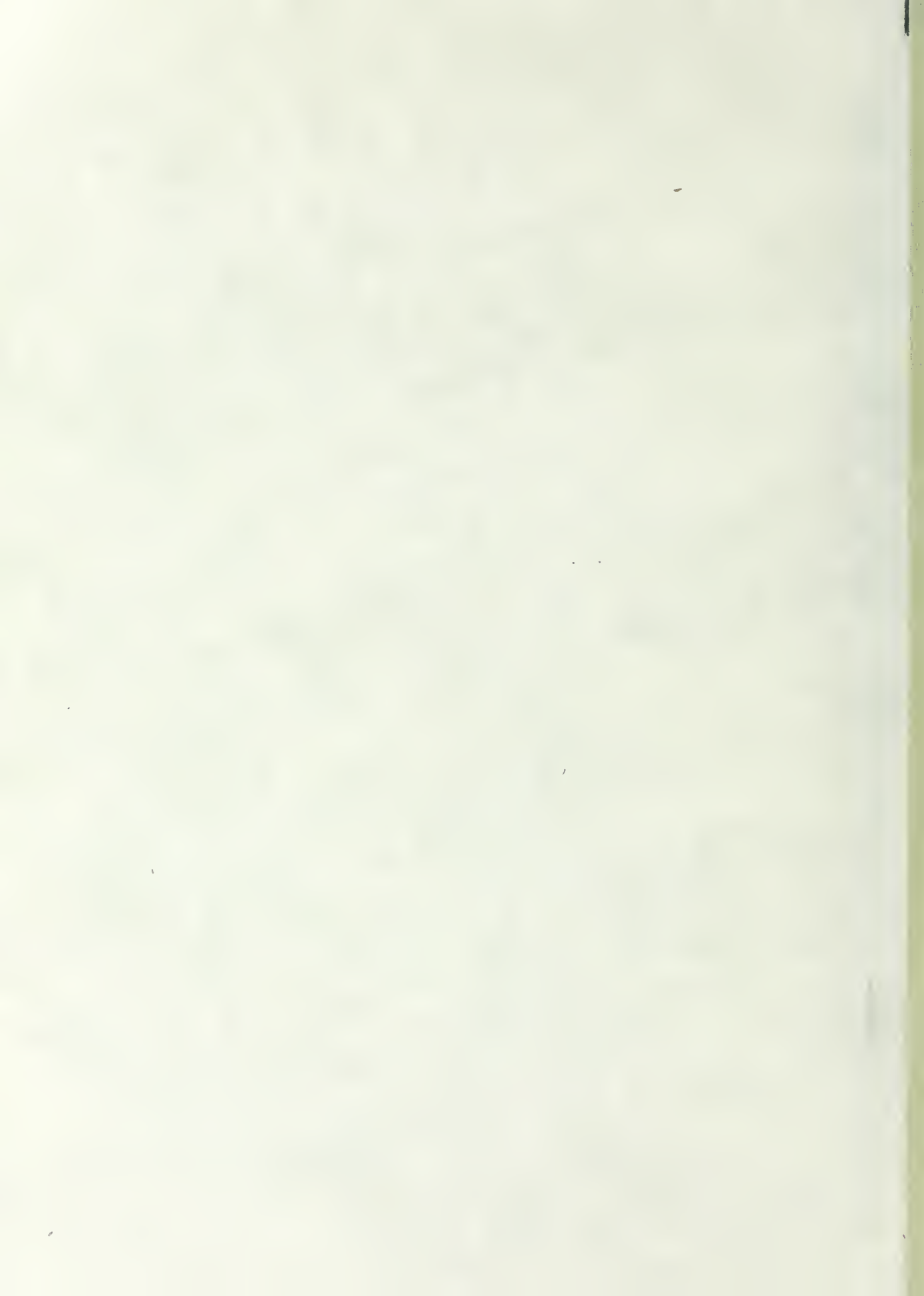


CERENKOV RADIATION PRODUCED BY
100 MeV ELECTRONS

David Earl McLaughlin



NAVAL POSTGRADUATE SCHOOL

Monterey, California



THESIS

CERENKOV RADIATION PRODUCED BY
100 MeV ELECTRONS

by

David Earl McLaughlin

June 1981

Thesis Advisor:

Fred R. Buskirk

Approved for public release; distribution unlimited

T200059

REPORT DOCUMENTATION PAGE		READ INSTRUCTIONS BEFORE COMPLETING FORM
1. REPORT NUMBER	2. GOVT ACCESSION NO.	3. RECIPIENT'S CATALOG NUMBER
4. TITLE (and Subtitle) Cerenkov Radiation Produced by 100 MeV Electrons		5. TYPE OF REPORT & PERIOD COVERED Master's Thesis; June 1981
7. AUTHOR(s) David Earl McLaughlin		6. PERFORMING ORG. REPORT NUMBER
9. PERFORMING ORGANIZATION NAME AND ADDRESS Naval Postgraduate School Monterey, California 93940		8. CONTRACT OR GRANT NUMBER(s)
11. CONTROLLING OFFICE NAME AND ADDRESS Naval Postgraduate School Monterey, California 93940		10. PROGRAM ELEMENT, PROJECT, TASK AREA & WORK UNIT NUMBERS
14. MONITORING AGENCY NAME & ADDRESS (if different from Controlling Office)		12. REPORT DATE June 1981
		13. NUMBER OF PAGES 48 pages
		15. SECURITY CLASS. (of this report) Unclassified
		16. DECLASSIFICATION/DOWNGRADING SCHEDULE
16. DISTRIBUTION STATEMENT (of this Report) Approved for public release; distribution unlimited		
17. DISTRIBUTION STATEMENT (of the abstract entered in Block 20, if different from Report)		
18. SUPPLEMENTARY NOTES		
19. KEY WORDS (Continue on reverse side if necessary and identify by block number) Stimulated Cerenkov radiation, superluminal, LINAC beam monitor.		
20. ABSTRACT (Continue on reverse side if necessary and identify by block number) It is proposed that electromagnetic radiation of a specified frequency can be produced as a result of stimulated Cerenkov radiation in a dielectric resonator excited by a superluminal electron beam. The frequency generated is a function of three physical parameters. They are the electron energy, the thickness of the dielectric resonator and its index of refraction. This work provides a theoretical derivation for predicting the frequency		

Item 20 (contd)

of stimulated Cerenkov radiation in a dielectric slab. The first experimental results using extremely relativistic electrons are reported, and the problems encountered are outlined with some suggestions for improvements. The results of this validation show that the observed frequency differs from the predicted frequency by less than 1.5%. Incidental to the conduct of this experiment, ordinary Cerenkov radiation in the usual cone was observed in air at microwave frequencies. A possible application of the stimulated Cerenkov process as an electron beam monitor is briefly discussed.

Approved for public release; distribution unlimited

Cerenkov Radiation Produced by
100 MeV Electrons

by

David Earl McLaughlin
Lieutenant Commander, United States Navy
B.S.M.E., Michigan State University, 1969

Submitted in partial fulfillment of the
requirements for the degree of

MASTER OF SCIENCE IN PHYSICS

from the

NAVAL POSTGRADUATE SCHOOL
June 1981

ABSTRACT

It is proposed that electromagnetic radiation of a specified frequency can be produced as a result of stimulated Cerenkov radiation in a dielectric resonator excited by a superluminal electron beam. The frequency generated is a function of three physical parameters. They are the electron energy, the thickness of the dielectric resonator and its index of refraction. This work provides a theoretical derivation for predicting the frequency of stimulated Cerenkov radiation in a dielectric slab. The first experimental results using extremely relativistic electrons are reported, and the problems encountered are outlined with some suggestions for improvements. The results of this validation show that the observed frequency differs from the predicted frequency by less than 1.5%. Incidental to the conduct of this experiment, ordinary Cerenkov radiation in the usual cone was observed in air at microwave frequencies. A possible application of the stimulated Cerenkov process as an electron beam monitor is briefly discussed.

TABLE OF CONTENTS

I. INTRODUCTION----- 9

II. THEORY-----11

III. EXPERIMENTAL EQUIPMENT AND PROCEDURE-----25

IV. DISCUSSION AND CONCLUSIONS-----38

APPENDIX A: NPS LINAC OPERATING CHARACTERISTICS-----41

APPENDIX B: TI-59 PROGRAM LISTING AND EXPLANATION-----42

LIST OF REFERENCES-----47

INITIAL DISTRIBUTION LIST-----48

LIST OF TABLES

I. Thicknesses of Polyethelyne for Modes 0,1,2-----	25
II. Frequencies Observed-----	36

LIST OF FIGURES

1. Coordinate System-----	12
2. Graphical Solution-----	17
3. Geometric Relationships-----	21
4. Dielectric Resonator-----	27
5. Air Cerenkov Experimental Setup-----	29
6. Vacuum Chamber-----	31
7. E-Field in the Dielectric-----	34
8. Vertical Conductor in Dielectric-----	35

ACKNOWLEDGEMENTS

The author wishes to express his gratitude to his thesis advisor, Professor Fred R. Buskirk, for his instruction, guidance and assistance in all phases of this project.

Thanks are also extended to Professor J. Knorr of the Naval Postgraduate School's Electrical Engineering Department for providing equipment and for his many helpful suggestions in the course of this work, and to Professor John E. Walsh of Dartmouth College for his encouragement.

The assistance of Mr. Don Snyder in the fabrication of the experimental setup and in the day-to-day operation and maintenance of the NPS LINAC is greatly appreciated.

Finally, the author wishes to thank his wife, Catherine, for her understanding, patience and support throughout this work and for her assistance in composition and proofreading.

I. INTRODUCTION

Cerenkov radiation, the radiation which is generated by a charged particle moving at superluminal velocity in a medium has been considered as a possible radiation source for many years. Additionally, Cerenkov radiation has been used as a charged particle detector which will selectively detect only charged particles exceeding the speed of light in the medium through which they are traveling. This detection is dependent upon only the velocity of the particle and the index of refraction of the medium. The detector is a simple photocell and as such does not distinguish between frequencies within its band of operability. Recently, Professor John E. Walsh [Ref. 1] reported successful generation of Cerenkov radiation using relativistic electrons and a dielectric resonator in the form of a cylindrical annulus. The import of Walsh's work is that the frequency of the radiation generated in the dielectric is a function only of the energy of the electrons, the thickness of the dielectric, and the index of refraction of the dielectric. Since these quantities are material parameters, it would appear that radiation of any desired frequency could be obtained by selecting the proper set of parameters.

The intent of this experiment is to extend Walsh's work, using a different geometry for the dielectric resonator and

much higher electron energies. Professor Walsh conducted his experiments at 300 KeV in contrast to the present experiment, which uses electron energies in the 10-100 MeV range, an increase of 1.5 to 2 orders of magnitude. In this experiment, radiation in the X band was selected for ease of measurement and analysis, with a view to extending the work into the IR range.

II. THEORY

Consider a dielectric slab with a coordinate system as shown in Figure 1. The dielectric has thickness h in the z direction and is unbounded in the x and y directions. There is a dielectric-conductor interface at $z=0$ which lies in the x - y plane. The dielectric slab has permittivity ϵ and permeability μ_0 while these quantities are ϵ_0 and μ_0 , respectively, in vacuum.

Starting with Maxwell's equations and following the usual procedure, it can be shown that the longitudinal components, E_x or H_x , satisfy a wave equation and the modes can be divided into TE or TM modes. The general expressions for the transverse components of the wave equation solution are:

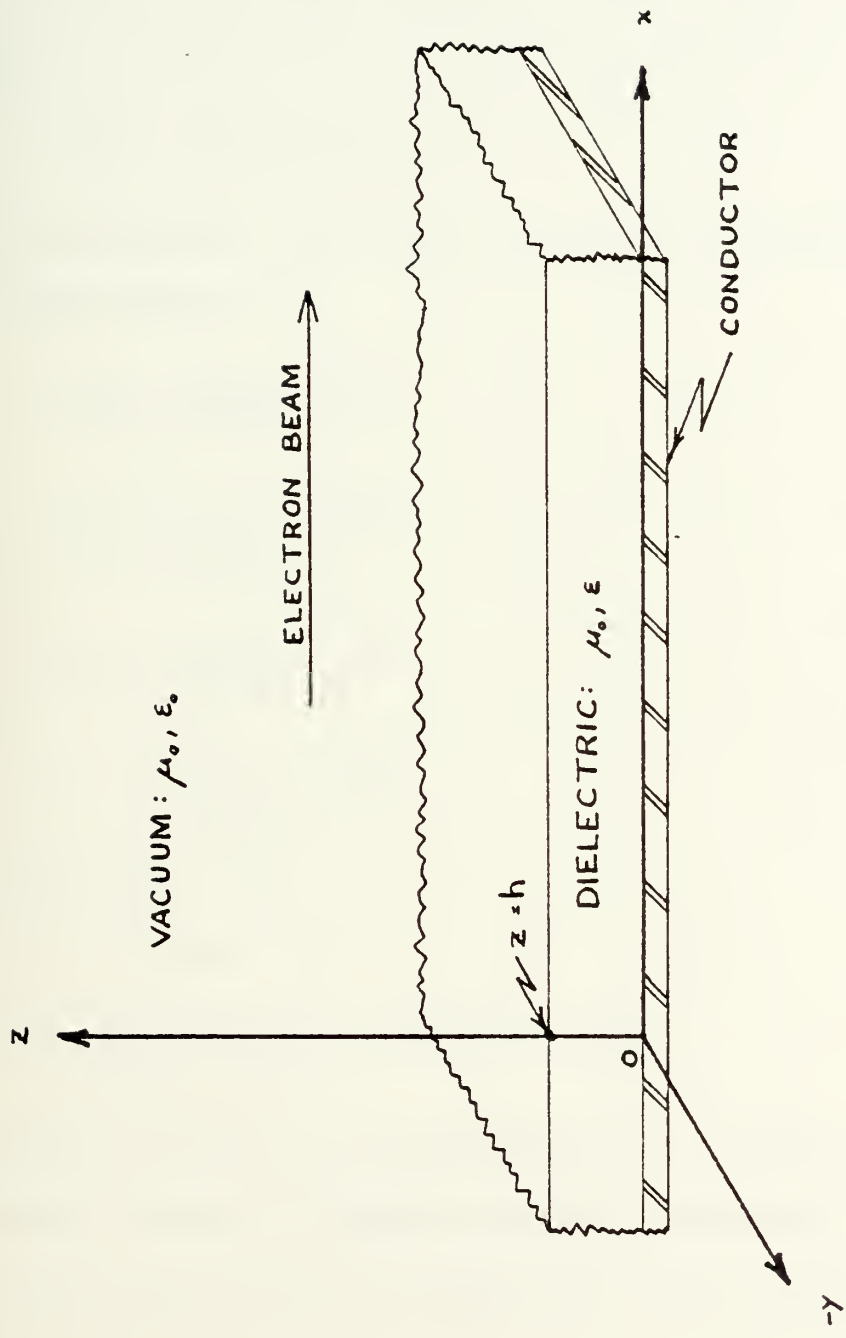
$$H_y = \frac{i\omega\epsilon}{\omega^2\mu\epsilon - k^2} \frac{\partial E_x}{\partial z} - \frac{ik}{\omega^2\mu\epsilon - k^2} \frac{\partial H_x}{\partial y} \quad (1)$$

$$F_z = \frac{-ik}{\omega^2\mu\epsilon - k^2} \frac{\partial E_x}{\partial z} + \frac{i\omega\mu}{\omega^2\mu\epsilon - k^2} \frac{\partial H_x}{\partial y} \quad (2)$$

$$E_y = \frac{-i\omega\mu}{\omega^2\mu\epsilon - k^2} \frac{\partial H_x}{\partial z} - \frac{ik}{\omega^2\mu\epsilon - k^2} \frac{\partial E_x}{\partial y} \quad (3)$$

$$H_z = \frac{-ik}{\omega^2\mu\epsilon - k^2} \frac{\partial H_x}{\partial z} - \frac{i\omega\epsilon}{\omega^2\mu\epsilon - k^2} \frac{\partial E_x}{\partial y} \quad (4)$$

The intent of this experiment is to take energy from a beam of electrons in the vacuum just above the dielectric slab



COORDINATE SYSTEM

FIGURE 1.

and give this energy to an EM wave in the slab and in the vacuum above the slab. This energy transfer requires a component of \vec{E} in the x-direction. Therefore, the wave in the dielectric should be TM mode. Thus, for TM modes where $H_x=0$ and E_x exist, the wave equation for E_x is:

$$(\nabla_{\perp}^2 + \{\omega^2\mu\epsilon - k^2\})E_x = 0 \quad (5)$$

When the condition that $H_x=0$ is applied to Equations 1, 2, 3 and 4, the result is

$$H_y = \frac{i\omega\epsilon}{\omega^2\mu\epsilon - k^2} \frac{\partial E_x}{\partial z} \quad (6)$$

$$E_z = \frac{-ik}{\omega^2\mu\epsilon - k^2} \frac{\partial E_x}{\partial z} \quad (7)$$

$$E_y = \frac{-ik}{\omega^2\mu\epsilon - k^2} \frac{\partial E_x}{\partial y} \quad (8)$$

$$H_z = \frac{-i\omega\epsilon}{\omega^2\mu\epsilon - k^2} \frac{\partial E_x}{\partial y} \quad (9)$$

For simplicity, let

$$\omega^2\mu_0\epsilon_0 - k^2 = -a^2 \quad (10)$$

for waves propagating in vacuum and let

$$\omega^2\mu_0\epsilon - k^2 = b^2 \quad (11)$$

for waves propagating in the dielectric. Assuming no y dependence, which is appropriate for a slab which extends to infinity in the + and - y directions, Eq. 5 reduces to

$$\frac{\partial^2 E_x}{\partial z^2} + (\omega^2\mu\epsilon - k^2)E_x = 0 \quad (12)$$

Thus, in vacuum, substituting Eq. 10 into Eq. 12 yields

$$\frac{\partial^2 E_x}{\partial z^2} - a^2 E_x = 0 \quad (13)$$

which, when the restriction that E_x goes to zero as z goes infinity is applied, has as its solution

$$E_x = Ae^{-az} \quad (14)$$

Similarly, substituting Eq. 11 into Eq. 12 for the dielectric case yields

$$\frac{\partial^2 E_x}{\partial z^2} + b^2 E_x = 0 \quad (15)$$

When the boundary condition of a conductor at the origin is imposed, the solution to Eq. 15 is

$$E_x = B \sin (bz) \quad (16)$$

At the vacuum-dielectric interface, the usual boundary conditions apply. That is, the tangential components of \vec{E} and \vec{H} must be continuous and the normal components of \vec{D} and \vec{B} must also be continuous. For this problem, with the given coordinate system, the tangential components of \vec{E} are E_x and E_y , the tangential components of \vec{H} are H_x and H_y . The normal component of $\vec{D} = \epsilon \vec{E}$ is ϵE_z and the normal component of $\vec{B} = (1/\mu) \vec{H}$ is $\frac{1}{\mu} H_z$. E_y and H_y are zero when the assumption of no y dependence is applied to Eqs. 8 and 9 and for TM modes H_x is zero by definition. Thus, the boundary conditions reduce to: E_x , H_y and ϵE_z must all be continuous at the

vacuum-dielectric interface. Equating Eqs. 14 and 16 at $z=h$ and applying the boundary condition of continuity to E_x leads to

$$Ae^{-ah} = B \sin (bh) \quad (17)$$

Making the appropriate substitutions into either Eqs. 6 or 7 and applying the continuity requirement for ϵE_z at $z=h$ results in the same equation.

$$\frac{i\omega\epsilon_0(-aAe^{-ah})}{-a^2} = \frac{i\omega\epsilon(bB \cos\{bh\})}{b^2} \quad (18)$$

This reduces to

$$\frac{\epsilon_0 A e^{-ah}}{a} = \frac{\epsilon B \cos(bh)}{b} \quad (19)$$

Equations 17 and 19 comprise a coupled set of equations which must be simultaneously satisfied.

The following development indicates one method of solution which leads to an expression for the propagation constant, k , and the corresponding phase velocity for the propagating mode. Dividing Eq. 17 by Eq. 19 gives

$$\frac{a}{\epsilon_0} = \frac{b}{\epsilon} \tan (bh) \quad (20)$$

$$\frac{\epsilon}{\epsilon_0} a = b \tan (bh) \quad (21)$$

$$\frac{\epsilon}{\epsilon_0} ah = bh \tan (bh) \quad (22)$$

Let $y=ah$ and $x=bh$

$$y = \frac{\epsilon_0}{\epsilon} x \tan x \quad (23)$$

Applying the definition of the index of refraction (n)

$$y = \frac{x \tan x}{n^2} \quad (24)$$

Recalling the definitions of a^2 and b^2 and adding them

$$a^2 + b^2 = \omega^2 \mu_0 (\epsilon - \epsilon_0) \quad (25)$$

$$a^2 h^2 + b^2 h^2 = \omega^2 \mu_0 (\epsilon - \epsilon_0) h^2 \quad (26)$$

Substituting for $(ah)^2$ and $(bh)^2$

$$y^2 + x^2 = \omega^2 \mu_0 (\epsilon - \epsilon_0) h^2 \quad (27)$$

The right hand side of Eq. 26 is a constant, which we will call R^2

$$y^2 + x^2 = R^2 \quad (28)$$

The simultaneous solution of Eqs. 23 and 28 for a given frequency will result in the value of k which yields fields satisfying all boundary conditions. A representative solution of this system of equations with $n=1.461$ (polyethylene) is shown in Figure 2.

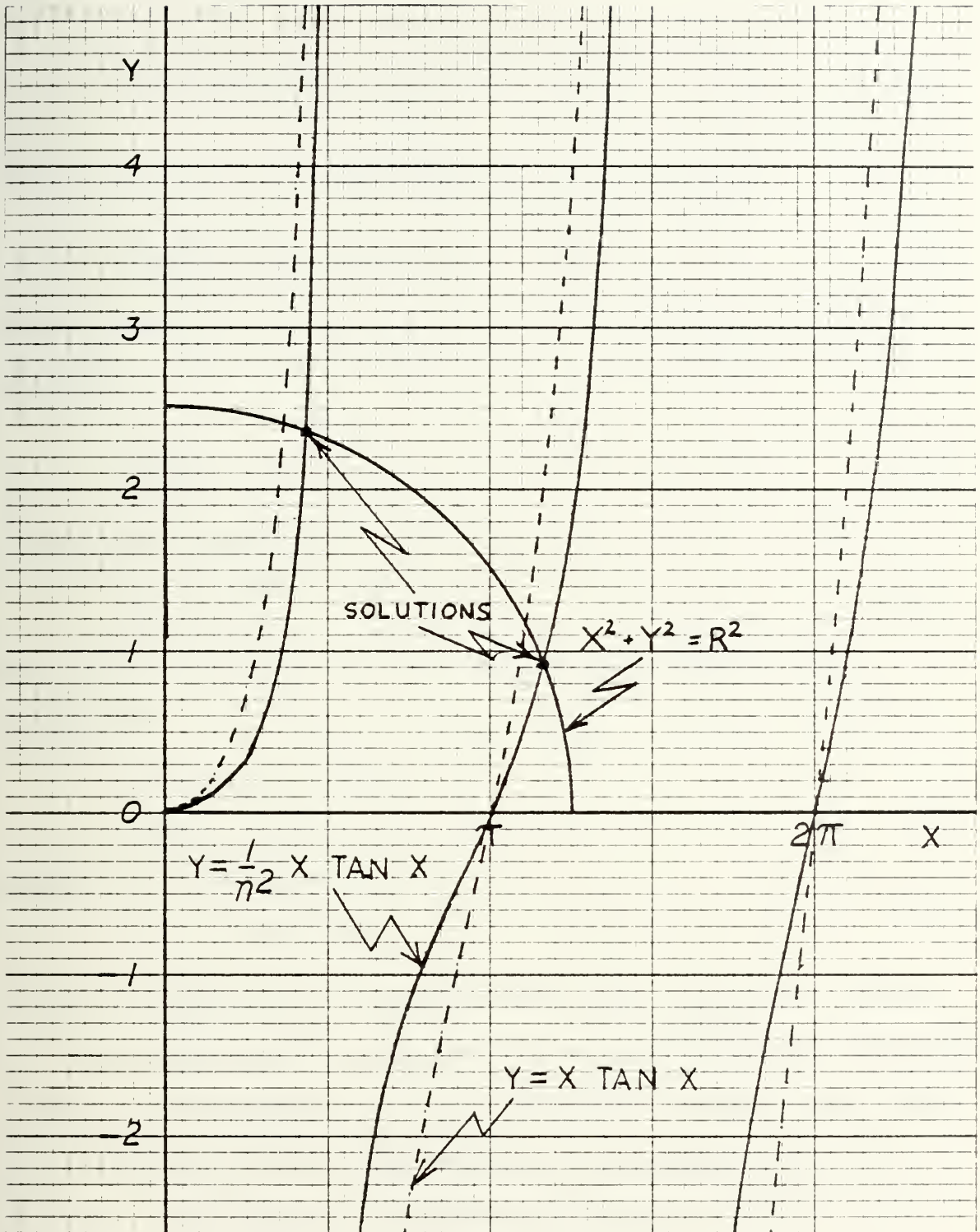
Although the TM modes are the desired modes, it is necessary to also consider the TE modes to see if there is any degeneracy. Equations 1, 2, 3 and 4 reduce to

$$H_Y = \frac{-ik}{\omega^2 \mu \epsilon - k^2} \frac{\partial H_X}{\partial y} \quad (29)$$

$$E_Z = \frac{i\omega\mu}{\omega^2 \mu \epsilon - k^2} \frac{\partial H_X}{\partial y} \quad (30)$$

$$E_Y = \frac{-i\omega\mu}{\omega^2 \mu \epsilon - k^2} \frac{\partial H_X}{\partial z} \quad (31)$$

$$H_Z = \frac{-ik}{\omega^2 \mu \epsilon - k^2} \frac{\partial H_X}{\partial z} \quad (32)$$



GRAPHICAL SOLUTION

FIGURE 2.

The TE mode wave equation for H_x is

$$(\nabla_{\perp}^2 + \{\omega^2 \mu \epsilon - k^2\}) H_x = 0 \quad (33)$$

Again, assuming no y dependence, Eq. 33 becomes

$$\frac{\partial^2 H_x}{\partial z^2} + (\omega^2 \mu \epsilon - k^2) H_x = 0 \quad (34)$$

Substituting Eq. 10 into Eq. 34 for waves propagating in vacuum

$$\frac{\partial^2 H_x}{\partial z^2} - a^2 H_x = 0 \quad (35)$$

which has a solution

$$H_x = C e^{-az} \quad (36)$$

and substituting Eq. 11 into Eq. 34 for waves in the dielectric

$$\frac{\partial^2 H_x}{\partial z^2} + b^2 H_x = 0 \quad (37)$$

which has a solution

$$H_x = D \sin (bz) \quad (38)$$

when the appropriate boundary condition at $z=0$ is imposed.

The same requirements for the vacuum-dielectric interface apply. The assumption of no y dependence immediately makes Eqs. 29 and 30 zero. The remaining tangential component of \vec{H} is H_x , the remaining tangential component of \vec{E} is E_y and for the normal components of \vec{D} and \vec{B} , only $B_z = \frac{1}{\mu} H_z$ remains. These three components must be continuous at the interface

at $z=h$. Thus

$$C e^{-ah} = D \sin (bh) \quad (39)$$

and

$$\frac{-i\omega\mu_0 (-aC e^{-ah})}{-a^2} = \frac{-i\omega\mu_0 (bD \cos \{bh\})}{b^2} \quad (40)$$

$$\frac{C e^{-ah}}{a} = \frac{D \cos (bh)}{b} \quad (41)$$

Dividing Eq. 39 by Eq. 41,

$$a = b \tan (bh) \quad (42)$$

$$ah = bh \tan (bh) \quad (43)$$

Again. letting $y=ah$ and $x=bh$,

$$y = x \tan x \quad (44)$$

Equations 27 and 28 are still valid and the simultaneous solution of Eqs. 28 and 44 will satisfy all boundary conditions for a given frequency.

The similarity between Eq. 44 and Eq. 23 indicates that both TE and TM modes will propagate at about the same frequency in the dielectric. However, only the TM mode is capable of gaining energy from the electrons. Accordingly, if stimulated Cerenkov radiation is observed, it will be the TM modes that are excited. If, however, an attempt is made to amplify waves fed into the dielectric from some outside source, some mechanism must be found to exclude the TE mode waves from being introduced into the dielectric.

A clearer picture of the relationships can be seen by use of geometry. First, define

$$k_f^2 = \omega^2 \mu_0 \epsilon_0 \quad (45)$$

the magnitude of the free space k vector for a plane wave and

$$k_d^2 = \omega^2 \mu_0 \epsilon \quad (46)$$

the magnitude of the k vector for a plane wave in the dielectric. Substituting these into Eqs. 10 and 11, the defining equations for a^2 and b^2 respectively, yields after multiplication by h^2 ,

$$k_f^2 h^2 - k^2 h^2 = -a^2 h^2 \quad (47)$$

$$k_d^2 h^2 - k^2 h^2 = b^2 h^2 \quad (48)$$

Subtracting Eq. 47 from Eq. 48

$$R^2 = h^2 k_d^2 - h^2 k_f^2 \quad (49)$$

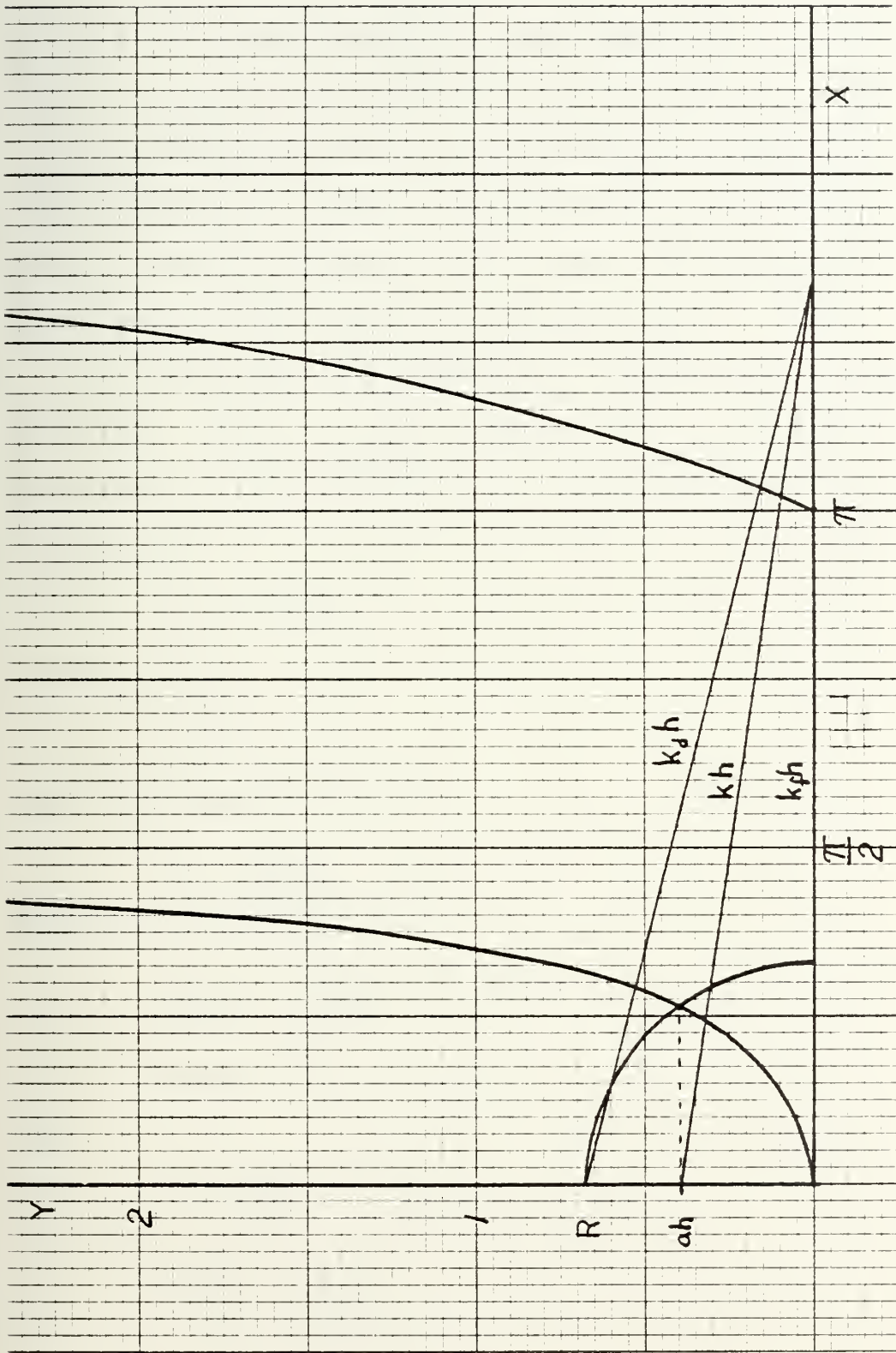
or

$$R^2 + h^2 k_f^2 = h^2 k_d^2 \quad (50)$$

This defines a right triangle as shown in Figure 2. Rearranging the terms in Eq. 47 defines another right triangle,

$$a^2 h^2 + k_f^2 h^2 = k^2 h^2 \quad (51)$$

also shown in Figure 3. Note that the side $k_f h$ is common to both triangles and that the magnitude of the unknown k , the wave number of the propagating mode in the dielectric that satisfies all the boundary conditions, is between k_f and k_d . There is an important consequence of this development.



GEOMETRIC RELATIONSHIPS

FIGURE 3.

Since, for energy exchange, the phase velocity of the wave in the dielectric, as represented by the unknown, k , must be matched to the velocity of the electrons. Also the velocity of the electrons must be less than the speed of light in the medium above the dielectric. Thus the region above the dielectric must be in vacuum because 100 MeV electrons have a velocity slightly faster than the velocity of a plane wave in air under normal conditions.

At this point it is possible to proceed to a numerical solution. First, by phase matching the velocity of the electrons to the velocity of the stimulated wave in the dielectric

$$v_{el} = v_{mode} \quad (52)$$

By definition

$$\beta = \frac{v}{c} \quad (53)$$

and after applying Eq. 52

$$\beta c = v_{mode} \quad (54)$$

Again, by definition

$$k_{mode} = \frac{\omega}{v_{mode}} \quad (55)$$

$$k_{mode} = \frac{\omega}{\beta c} \quad (56)$$

and

$$\gamma^2 = \frac{1}{1-\beta^2} \quad (57)$$

$$\beta^2 = \left(1 - \frac{1}{\gamma^2}\right) \quad (58)$$

Substituting Eq. 58 into Eq. 56

$$k_{\text{mode}} = \frac{\omega}{\left(1 - \frac{1}{\gamma^2}\right)^{\frac{1}{2}} c} \quad (59)$$

Thus, k_{mode} is determined for a given γ and ω . Once ω is specified, Eqs. 45 and 46 specify k_f and k_d . Rearranging Eq. 10 and substituting Eq. 45 yields

$$a^2 = k_{\text{mode}}^2 - k_f^2 \quad (60)$$

$$a = (k_{\text{mode}}^2 - k_f^2)^{\frac{1}{2}} \quad (61)$$

Similarly

$$b^2 = (k_d^2 - k_{\text{mode}}^2) \quad (62)$$

$$b = (k_d^2 - k_{\text{mode}}^2)^{\frac{1}{2}} \quad (63)$$

Solving Eq. 21 for h

$$\frac{\epsilon a}{\epsilon_0} = b \tan (bh) \quad (21)$$

$$\frac{\epsilon a}{\epsilon_0 b} = \tan (bh) \quad (64)$$

$$bh = \tan^{-1} \left(n^2 \frac{a}{b} \right) \quad (65)$$

$$h = \frac{1}{b} \tan^{-1} \left(n^2 \frac{a}{b} \right) \quad (66)$$

Thus, given a desired frequency, ω , the index of refraction of the dielectric, n , and the energy of the electrons, γ , the thickness of the dielectric can be determined.

The substitution of Eq. 59 into Eqs. 10 and 11 allows the factoring out of ω^2 and Eq. 66 becomes

$$h = \frac{1}{\omega \left(\mu_0 \epsilon - \frac{1}{\left(1 - \frac{1}{\gamma^2}\right) c^2} \right)^{\frac{1}{2}}} \tan^{-1} \left\{ n^2 \frac{\left(\frac{1}{\left(1 - \frac{1}{\gamma^2}\right) c^2} - \mu_0 \epsilon \right)^{\frac{1}{2}}}{\left(\mu_0 \epsilon - \frac{1}{\left(1 - \frac{1}{\gamma^2}\right) c^2} \right)^{\frac{1}{2}}} \right\} \quad (67)$$

which can be solved for ω given h , n , and γ .

$$\omega = \frac{1}{h \left(\mu_0 \epsilon - \frac{1}{\left(1 - \frac{1}{\gamma^2}\right) c^2} \right)^{\frac{1}{2}}} \tan^{-1} \left\{ n^2 \frac{\left(\frac{1}{\left(1 - \frac{1}{\gamma^2}\right) c^2} - \mu_0 \epsilon \right)^{\frac{1}{2}}}{\left(\mu_0 \epsilon - \frac{1}{\left(1 - \frac{1}{\gamma^2}\right) c^2} \right)^{\frac{1}{2}}} \right\} \quad (68)$$

The significance of Eq. 68 is that the physical parameters of h , n , and γ specify ω . With the proper selection of these parameters, EM radiation of any frequency can be generated.

Examination of Figure 2 readily shows that if the dimensionless parameter bh exceeds π , more than one solution is possible. However, these modes will be at different frequencies and the graphical solution indicates that, if $x < 3\pi$, the single desired frequency can be extracted by use of a band-pass or high pass filter.

III. EXPERIMENTAL EQUIPMENT AND PROCEDURE

It was decided to conduct this experiment in the X-band (8-12 GHz) after consulting with Professor Knorr and investigating the availability of the necessary equipment and measuring devices needed to support the experiment. The dielectric chosen was polyethelyne which has an index of refraction of 1.461 [Ref. 2]. The Naval Postgraduate School's Linear Accelerator (LINAC) is capable of producing relativistic electrons with energies up to 120 MeV. The operating characteristics of the NPS LINAC can be found in Appendix A.

A TI-59 programmable calculator program was developed to solve Eqs. 67 and 68. An explanation of this program and a listing of it can be found in Appendix B. Table I shows the input parameter values and the program's solution of Eq. 66 for the 0, 1 and 2 modes.

TABLE I

THICKNESSES OF POLYETHELYNE FOR MODES 0,1,2

m	E [MeV]	n	f [FHZ]	h[mm] ¹
0	50	1.461	10	.095
1	50	1.461	10	14.07
2	50	1.461	10	28.15

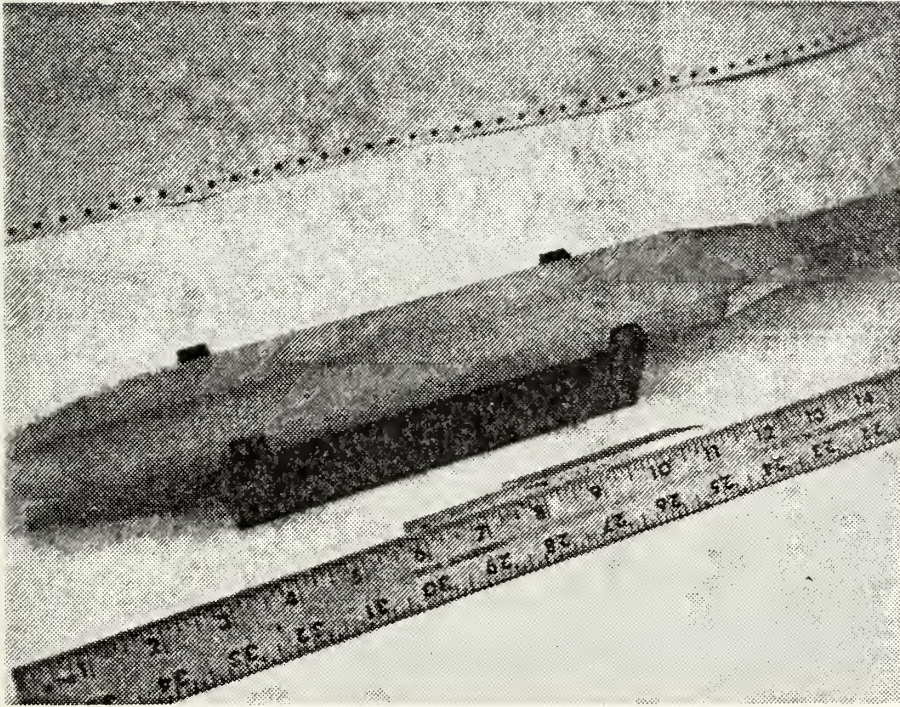
¹Program output value

Based on these results, a thickness of 12.7mm (0.5 in) was selected. The values of $E=50$ MeV, $n=1.461$, $h=12.7$ mm for a Mode 1 solution predict a frequency of 11.08 GHz when the TI-59 program solves Eq. 68.

The beam of the LINAC is approximately 1 cm in diameter. The width of the dielectric was made to be 5.08 cm to approximate the infinite slab in the y direction. The end of the dielectric away from the LINAC exit window was tapered to fit into an X-band hollow waveguide and to facilitate the TM to TE transition required since a TE mode is the lowest mode that will propagate in a hollow waveguide. Figure 4 is a photograph of the dielectric resonator as it was originally configured.

The first attempt to observe the desired EM radiation met with only limited success. The dielectric slab was mounted about 1 cm below the centerline axis of the LINAC exit window in air. The metal waveguide was sloped slightly to allow clear passage of the electrons over the top of the flange connector to the detector. A diode detector was used with its output lead to an oscilloscope (CRO). With a beam energy of 53.85 MeV and an average beam current² of 8.0 nAmp, the CRO display showed a pulse of about 1 μ sec with strength varying from 100-200 mV as the beam was tuned, focused and

²All currents read on a secondary emission monitor with 6% efficiency, and the monitor current is reported in this work.



DIELECTRIC RESONATOR

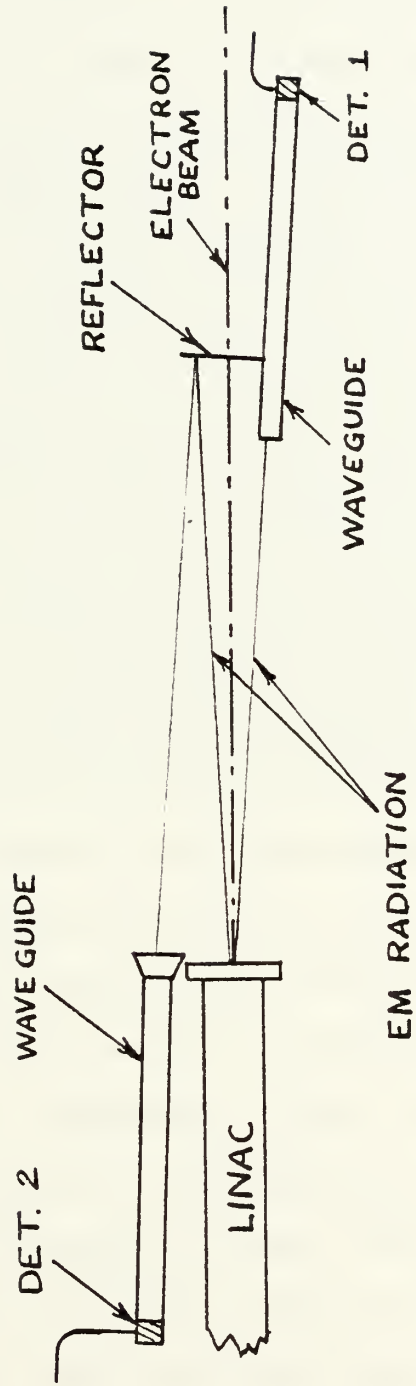
FIGURE 4.

varied in distance from the slab. However, attempts to measure the frequency with a high Q calibrated cavity resonator were unsuccessful.

To determine if the observed pulse was caused by the dielectric, the slab was removed leaving the hollow waveguide in place. When the beam was turned on, a 0.5 microsecond pulse of slightly reduced magnitude was observed. At this point, it was realized that the observed pulse might be caused by Cerenkov radiation in air. Although commonly accepted as 1.0, the actual index of refraction of standard dry air is 1.003 [Ref. 3]. Using this value as β^{-1} it can be easily shown that electrons with energies exceeding 20.856 MeV will exceed the speed of light in standard dry air. Thus, electrons above that energy would exceed the velocity of a plane wave in air, and could not be matched to the TM mode velocity.³

A simple experiment was designed to investigate this possibility. The equipment arrangement is shown in Figure 5. The reflector used was a thin sheet of aluminum which would allow the passage of the electrons and reflect any EM radiation. With the reflector in place, a pulse was observed from detector 2 whose magnitude was approximately 0.5 times the magnitude of the output from detector 1. When the reflector was removed, a pulse of magnitude 0.1 times the output of

³See Section II.



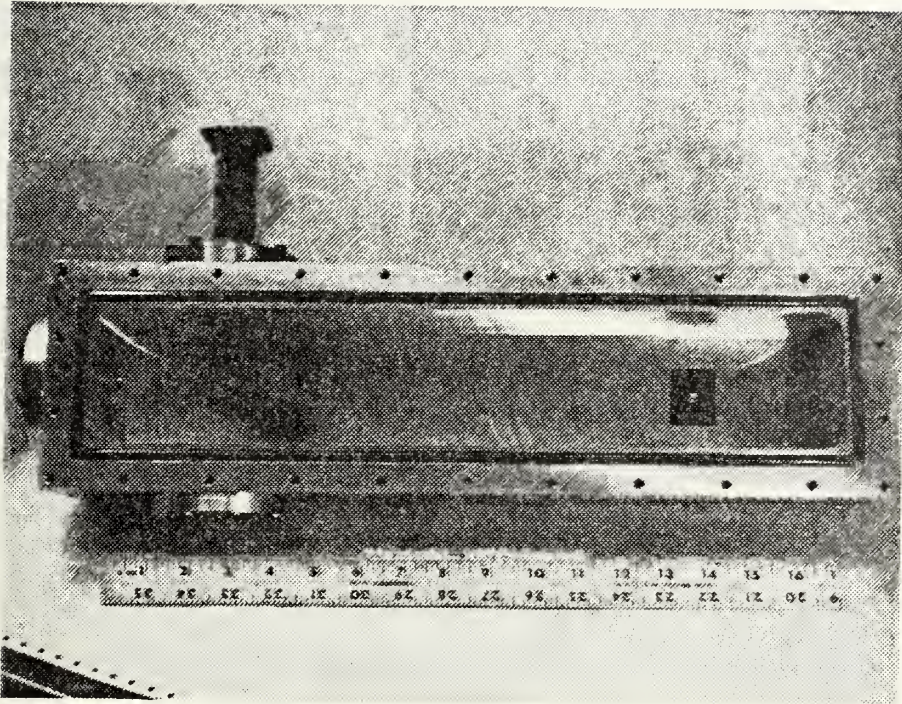
AIR CERENKOV EXPERIMENTAL SETUP

FIGURE 5.

detector 1 was observed from detector 2. These results support the hypothesis of air Cerenkov. Since the air Cerenkov should be very broadband, no attempt was made at this time to measure the frequency of this radiation.

Based on these results, it was decided to enclose the dielectric slab in a vacuum chamber. Figure 6 is a photograph of the interior of the vacuum chamber. The vacuum was maintained in the chamber by installing a 1/16 in. thick piece of polyethylene between two waveguide flanges exterior to the chamber. A waveguide run of about 75 ft. was added to the setup which allowed for the positioning of the detector in the LINAC control room thus eliminating the long, lossy coaxial cable runs. A Tektronic 491 Spectrum Analyzer (491-S/A) was obtained to facilitate frequency analysis.

The use of this new setup with beam energy of 100.97 MeV, beam current of 4.3 nA and the same diode detector used before resulted in a 0.5 Volt peak pulse of about 1 microsecond duration. The increase in peak output was attributed to the reduction in line loss provided by the replacement of the coax cable by waveguide. Subsequent tests, which will be discussed later, have modified this hypothesis. The 491-S/A, with a 20 dB attenuator inserted between the waveguide to coax adapter and the S/A, detected signals at 12.39 GHz and 8.57 GHz. The 12.39 GHz signal was the image of a real signal above the frequency range of the 491-S/A. Using a relatively low Q cavity, it was determined that most of the



VACUUM CHAMBER

FIGURE 6.

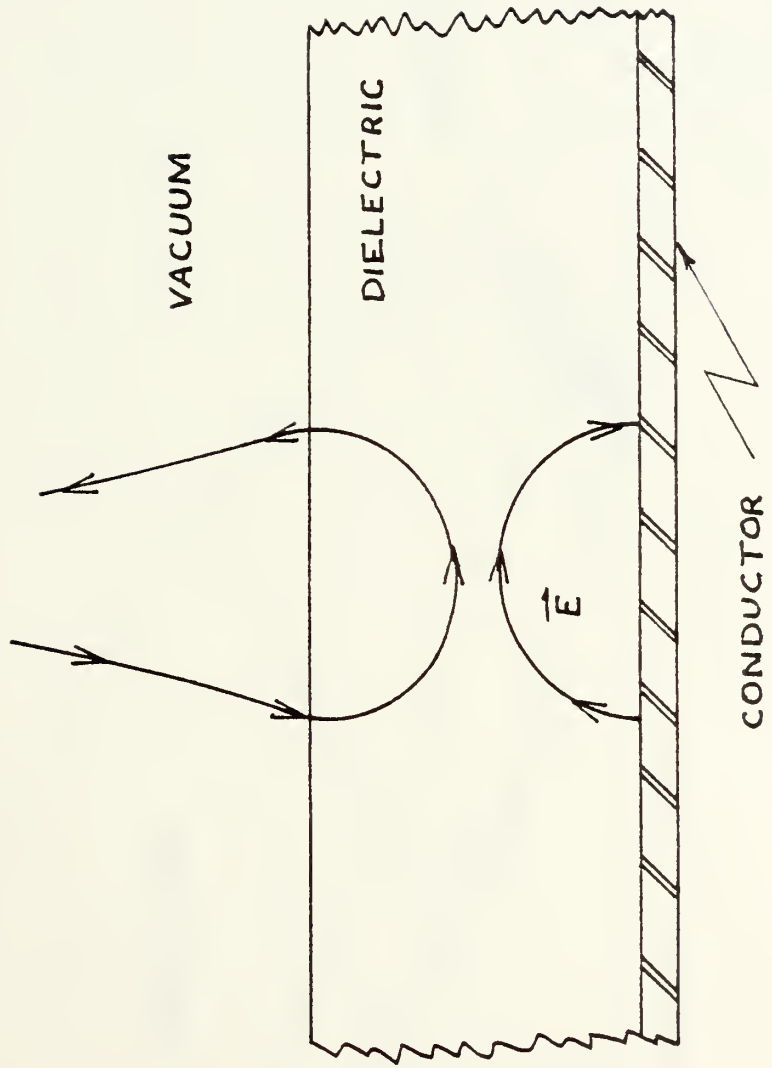
power in the pulse was in the 8.57 GHz signal. A dispersive high pass filter with a cutoff frequency of 9.9 GHz was installed between the waveguide from the dielectric and the coax adapter. With this arrangement and no attenuation at the input of the 491-S/A, valid signals were detected at 8.58, 8.99 and 11.42 GHz. When the dielectric was removed from the vacuum chamber and the test repeated, the same signals were detected. Both with and without dielectric, all signals disappeared when electron injection was interrupted with LINAC RF power maintained.

The 8.57 GHz and 11.48 GHz signals appear to be the third and fourth harmonics of the LINAC operating frequency. The exact cause of the 8.99 GHz signal is not known but it is believed to be caused by a resonant mode of the vacuum chamber. The chamber is a rectangular aluminum box with 10 mil aluminum windows for electron entry and exit and as such would act as a cavity resonator. Equipment limitations prevent the measurement of any change in strength of the 11.48 GHz signal with and without the dielectric slab in place. This frequency is only 4% above the predicted frequency for the given parameters and it is possible that the desired signal is hidden by the LINAC harmonic at that frequency. Also, the actual index of refraction of the polyethylene was not experimentally determined and it was not manufactured specifically for optical use. It is possible that a slight change in n and/or inhomogeneities in the material could cause some frequency shifting.

Additional tests were conducted with this configuration. Two anomalies were observed which required further explanation. First, an intermittent, valid signal was detected at 10.24 GHz. This signal is not fully understood but it is believed to be extraneous to the experiment. Secondly, the peak output of the diode detector varied as much as an order of magnitude with the same beam parameters and beam position.

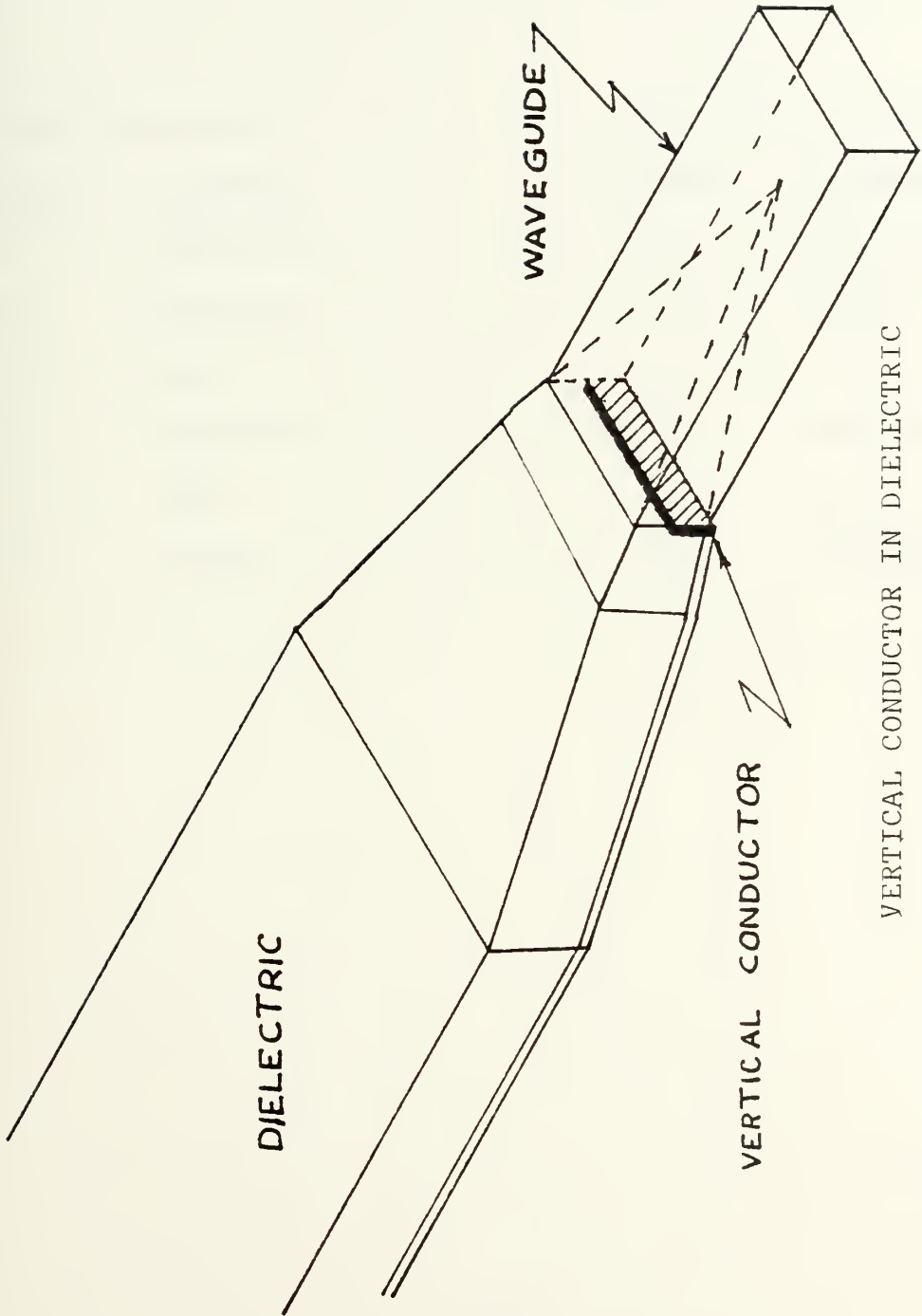
This observation led to a more intensive investigation of the TM to TE coupling at the dielectric/waveguide transition. In particular, for the $m=1$ mode, it was realized that cancellation of the E-field could occur at the transition point. A graphical representation of the E-field in the dielectric is shown in Figure 7. It was decided to nullify the lower field at the transition by inserting a vertical conductor into the dielectric slab at the mouth of the waveguide as shown in Figure 8. The vertical conductor should not affect any TE modes propagating in the dielectric but should nullify the cancellation effect of the $m=1$ mode for any TM mode waves propagating in the dielectric. Another modification of the setup was also made at this time. The 10 mil. aluminum window between the LINAC and the vacuum chamber was replaced by a 10 mil. mylar window to minimize beam spreading at the entrance to the vacuum chamber.

Table II shows the results of the frequency analysis of the dielectric with and without the conductor in place. The beam parameters were as follows: $E=65.29$ MeV, $I=4.0$ nA.



E-FIELD IN THE DIELECTRIC

FIGURE 7.



VERTICAL CONDUCTOR IN DIELECTRIC

FIGURE 8.

TABLE II
FREQUENCIES OBSERVED

With Conductor		Without Conductor	
<u>f [GHz]</u>	<u>Strength</u>	<u>f [GHz]</u>	<u>Strength</u>
8.57	very strong	8.57	strong
9.00	moderate	9.00	weak
9.52	weak	----	----
10.21	moderate	10.25	moderate
10.92	weak	----	----
11.42	strong	11.50	moderate

The peak voltage observed from the diode detector was 150 mV without the vertical conductor and 100 mV with the conductor in place. It is interesting to note that although half of the area of the waveguide was blocked, the detector voltage dropped by only about one third.

For input values of $E=65.29$ MeV, $n=1.461$, $h=12.7$ mm and $m=1$, the TI-59 program predicts a frequency of 11.08 GHz. The 9.52 GHz signal does not correspond to any predicted frequency. Possible explanations of this frequency will be discussed later. The observed 10.92 GHz signal is only 1.4% below the predicted value. Since this frequency is only observed when the vertical conductor is in place, it is believed that this is a TM mode resulting from stimulated Cerenkov radiation.

IV. DISCUSSION AND CONCLUSIONS

It appears from the foregoing experiment that stimulated Cerenkov radiation can be produced at the predicted frequency with the proper choice of parameters. The 1.4% error can be explained in several ways. First, the predicted frequency is based on an algorithm that provides an approximate solution for modes where $m > 0$. Second, nonoptical quality polyethylene was used for the dielectric slab. Finally, the theoretical development assumed an infinite slab in the y direction. In fact, a finite slab was used whose y dimension was about 5 times the diameter of the focused beam. Any one of the deviations from the ideal case or a combination of them could account for the error. The most probable source of error is the index of refraction of the polyethylene. An index of refraction of 1.473, a change of 0.012 which is less than 1% of the tabulated value in Ref. 3, would reduce the error to essentially zero.

The cause of the TM mode frequency at 9.52 GHz shown in Table II is not fully understood. It could be a result of the edge effects caused by the finite width of the dielectric or it might be a resonant TM mode of the vacuum chamber.

A secondary effect observed during the course of this experiment is worth noting. When the focused beam was passed above the dielectric, the output of the diode detector

varied with the beam current. This effect was present both in air and in vacuum. It may be possible to construct a calibration curve of diode voltage vs. beam current and thereby develop a beam current measuring device which does not destroy the beam downstream from the measurement point as the beam current measuring device presently in use does.

It is readily apparent from the magnitude of the diode pulse that the stimulated Cerenkov radiation effect is very inefficient. To match the mode with high speed electrons requires that the component of the mode's E-field parallel to the electron beam be small compared with the field's transverse components. This will tend to make the coupling small. The output power of the diode detector is less than 0.5 mWatts. Most of this power, conservatively estimated at 95%, is in the 8.57 GHz signal as demonstrated in Section III. This does, however, enhance the possibility of developing an electron beam current meter, based on this process, which has only a minimal effect on the beam itself.

The results of this experiment support the hypothesis that stimulated Cerenkov radiation can be produced at a frequency specified by the physical parameters of electron energy, index of refraction and dielectric thickness. It appears that the wave-electron coupling is a weak effect which is further degraded by the TM to TE coupling used to extract the signal in this experiment. Greater efficiency may be possible if a more effective means of extracting the

signal is developed. The signal itself may be increased in strength by lengthening the dielectric slab to increase the length of the wave-electron interaction region.

Additional work in the area of stimulated Cerenkov radiation appears to be warranted. The development presented here is not guaranteed to be unique. There may be other modes that can be stimulated in the dielectric, one of which might provide a stronger signal. A mode with a larger longitudinal component could increase the electron-mode coupling. Additionally, the effect of the pulsed beam of electrons should be studied in depth. Specifically, the question of why this experimental setup produces most of its output power at the third harmonic of the LINAC operating frequency should be investigated in greater detail. If the power in the LINAC harmonics can be shifted to the Cerenkov frequency it would greatly increase the usefulness of the stimulated Cerenkov process as a radiation source. Finally, generation of X-band radiation using the $m=0$ mode should be attempted as a preliminary step in extending this work into the IR range. The dielectric thickness predicted by the theoretical development presented here for an IR generator is of the order of microns. The X-band $m=0$ thickness is in this range. Extracting a signal from a dielectric this thin may cause some difficulties. The experience thus gained should be valuable in extending this work into the IR range.

APPENDIX A

LINAC OPERATING CHARACTERISTICS

Max Energy	120 MeV
Max Average Current	3-5 microAmp
Operating Frequency	2.856 GHz
PRF	60 pps
Pulse Duration	1.0 microseconds
Nr. of Klystrons	3
Peak Output Power per Klystron	21 MWatts

APPENDIX B

TI-59 PROGRAM LISTING AND EXPLANATION

This program does not use any library programs within the algorithm. The inputs are the electron beam energy (in MeV), the index of refraction of the dielectric (dimensionless), either the desired frequency (in Hz) or the dielectric thickness (in meters), and the mode (dimensionless). The mode input determines which leg of the $y=(1/n^2)x \tan x$ in the curve (in the first quadrant) is used. For a given $m=0,1,2\dots$ the solution is found for x values such that $m\pi < x < [(2m+1)\pi/2]$. As noted in Chapter II, if $x > \pi$, more than one solution is possible. This program solves only for the solution in the $m\pi < x < [(2m+1)\pi/2]$ range.

The solution for $m=0$ is unique and exact. Solutions for higher order modes are found using an iterative search. The solution is approximate in that the program searches down the designated leg of $y=(1/n^2)x \tan x$ in discrete steps until it finds a y value less than the y value for the corresponding $m=0$ case. This value of y is then taken as the solution point for the input mode.

To solve Equation 67:

1. Load program.
2. Enter E[MeV], press A.

3. Enter n , press B.
4. Enter $f[nz]$, press C.
5. Enter m , press E.

The program will solve for h [meters].

To solve Equation 68:

1. Load program.
2. Enter $E[\text{MeV}]$, press A.
3. Enter n , press B.
4. Enter $h[\text{m}]$, press D.
5. Enter m , press E'.

The program will solve for $f[\text{Hz}]$.

The program listing is on the following pages.

000	76	LBL	049	65	X	098	42	STO
001	11	A	050	89	π	099	18	18
002	57	ENG	051	95	=	100	91	R/S
003	55	\div	052	42	STO	101	76	LBL
004	93	.	053	05	05	102	18	C7
005	05	5	054	91	R/S	103	01	1
006	01	1	055	76	LBL	104	42	STO
007	01	1	056	14	D	105	05	05
008	95	=	057	42	STO	106	71	SBR
009	42	STO	058	06	06	107	88	DMS
010	00	00	059	91	R/S	108	71	SER
011	91	R/S	060	76	LBL	109	69	OP
012	76	LBL	061	15	E	110	55	\div
013	12	B	062	42	STO	111	02	2
014	33	x^2	063	07	07	112	55	\div
015	42	STO	064	67	EQ	113	89	π
016	01	01	065	19	D'	114	95	=
017	65	X	066	71	SBR	115	91	R/S
018	08	8	067	88	DMS	116	76	LBL
019	93	.	068	71	SBR	117	19	D'
020	08	8	069	68	NOP	118	71	SBR
021	05	5	070	43	RCL	119	88	DMS
022	04	4	071	13	13	120	71	SBR
023	01	1	072	65	X	121	68	NOP
024	01	1	073	43	RCL	122	91	R/S
025	08	8	074	11	11	123	76	LBL
026	52	EE	075	95	=	124	10	E'
027	94	+/-	076	42	STO	125	42	STO
028	01	1	077	14	14	126	07	07
029	02	2	078	71	SBR	127	67	EQ
030	42	STO	079	58	FIX	128	18	C'
031	02	02	080	42	RCL	129	01	1
032	95	=	081	15	15	130	42	STO
033	42	STO	082	33	x^2	131	05	05
034	03	03	083	85	+	132	71	SBR
035	04	4	084	43	RCL	133	88	DMS
036	52	EE	085	17	17	134	71	SBR
037	94	+/-	086	33	x^2	135	69	OP
038	07	7	087	95	=	136	43	RCL
039	65	X	088	55	\div	137	08	08
040	89	π	089	53	(138	75	-
041	95	=	090	43	RCL	139	43	RCL
042	42	STO	091	10	10	140	09	09
043	04	04	092	75	-	141	95	=
044	91	R/S	093	43	RCL	142	34	\sqrt{x}
045	76	LBL	094	09	09	143	65	X
046	13	C	095	54)	144	43	RCL
047	65	X	096	95	=	145	19	19
048	02	2	097	34	\sqrt{x}	146	65	X

147	43	RCL	196	93	.	245	34	\sqrt{x}
148	06	06	197	09	9	246	42	STO
149	95	=	198	09	9	247	11	11
150	42	STO	199	07	7	248	43	RCL
151	14	14	200	09	9	249	10	10
152	71	SBR	201	02	2	250	75	-
153	58	FIX	202	05	5	251	43	RCL
154	43	RCL	203	52	EE	252	08	08
155	15	15	204	08	8	253	95	=
156	33	x^2	205	33	x^2	254	34	\sqrt{x}
157	85	+	206	95	=	255	42	STO
158	43	RCL	207	35	1/x	256	12	12
159	17	17	208	65	X	257	92	RTN
160	33	x^2	209	43	RCL	258	76	LBL
161	95	=	210	05	05	259	68	NOP
162	55	\div	211	33	x^2	260	43	RCL
163	43	RCL	212	95	-	261	01	01
164	06	06	213	42	STO	262	65	X
165	33	x^2	214	08	08	263	43	RCL
166	55	\div	215	43	RCL	264	11	11
167	53	(216	05	05	265	55	\div
168	43	RCL	217	33	x^2	266	43	RCL
169	10	10	218	65	X	267	12	12
170	75	-	219	43	RCL	268	95	=
171	43	RCL	220	02	02	269	70	RAD
172	09	09	221	65	X	270	22	INV
173	54)	222	43	RCL	271	30	TAN
174	95	=	223	04	04	272	55	\div
175	34	\sqrt{x}	224	95	=	273	43	RCL
176	42	STO	225	42	STO	274	12	12
177	20	20	226	09	09	275	95	=
178	55	\div	227	43	RCL	276	42	STO
179	02	2	228	05	05	277	13	13
180	55	\div	229	33	x^2	278	92	RTN
181	89	π	230	65	X	279	76	LBL
182	95	=	231	43	RCL	280	69	OP
183	91	R/S	232	03	03	281	43	RCL
184	76	LBL	233	65	X	282	01	01
185	88	DMS	234	43	RCL	283	65	X
186	43	RCL	235	04	04	284	43	RCL
187	00	00	236	95	=	285	11	11
188	33	x^2	237	42	STO	286	55	\div
189	35	1/x	238	10	10	287	43	RCL
190	94	+/-	239	43	RCL	288	12	12
191	85	+	240	08	08	289	95	=
192	01	1	241	75	-	290	70	RAD
193	95	=	242	43	RCL	291	22	INV
194	65	X	243	09	09	292	30	TAN
195	02	2	244	95	=	293	55	\div

294 53 (
295 43 RCL
296 12 12
297 65 X
298 43 RCL
299 06 06
300 54)
301 95 =
302 42 STO
303 19 19
304 92 RTN
205 76 LBL
306 58 FIX
207 09 9
308 94 +/-
309 22 INV
310 28 LOG
311 85 +
312 43 RCL
313 07 07
314 65 X
315 89 π
316 95 =
317 42 STO
318 15 15
319 01 1
320 01 1
321 94 +/-
322 22 INV
232 28 LOG
324 94 +/-
325 42 STO
326 16 16
327 76 LBL
328 50 $|x|$
329 43 RCL
330 15 15
331 70 RAD
332 30 TAN
333 65 X
334 43 RCL
335 15 15
336 55 \div
337 43 RCL
338 01 01
339 95 =
340 42 STO
341 17 17
342 75 -

343 43 RCL
344 14 14
345 95 =
346 22 INV
347 77 GE
348 59 INT
349 43 RCL
350 16 16
351 44 SUM
352 15 15
353 61 GTO
354 50 $|x|$
355 76 LBL
356 59 INT
357 92 RTN

LIST OF REFERENCES

1. Walsh, J. E., "Stimulated Cerenkov Radiation," Physics of Quantum Electronics, Vol. 5, Ed. S. F. Jacobs et al, Addison Wesley Publishing Company, Inc., 1978.
2. Simonis, G. J., "Near mm Wave Materials," Harry Diamond Labs.
3. Hodgman, C. D., Handbook of Chemistry and Physics, 38th Edition, Chemical Rubber Publishing Co., 1956.

INITIAL DISTRIBUTION LIST

	No. Copies
1. Defense Technical Information Center Cameron Station Alexandria, Virginia 22314	2
2. Library, Code 0142 Naval Postgraduate School Monterey, California 93940	2
3. Physics Library, Code 61 Department of Physics and Chemistry Naval Postgraduate School Monterey, California 93940	1
4. Professor F. R. Buskirk, Code 61Bs Department of Physics and Chemistry Naval Postgraduate School Monterey, California 93940	5
5. LCDR David E. McLaughlin, USN 1062 Clearspring Lane Virginia Beach, Virginia 23464	1

Thesis
M238
c.1

McLaughlin

Cerenkov radiation
produced by 100 MeV
electrons.

193680

OCT 21 85

3 APR 86
16 NOV 87

33067

30635
33326

Thesis
M238
c.1

McLaughlin

Cerenkov radiation
produced by 100 MeV
electrons.

193680

thesM238

Cerenkov radiation produced by 100 MeV e



3 2768 001 88245 9

DUDLEY KNOX LIBRARY